

Optical Properties of Fluorinated Polyimides and Their Applications to Optical Components and Waveguide Circuits

Shinji ANDO*

Department of Organic & Polymeric Materials, Tokyo Institute of Technology,

Ookayama, Meguro-ku, Tokyo, 152-8552, Japan

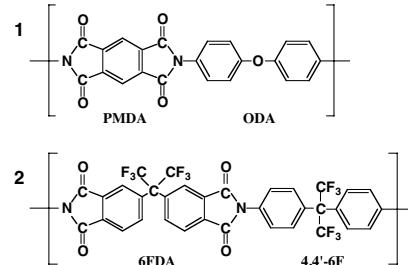
e-mail : sando@polymer.titech.ac.jp

This article reviews the optical properties of fluorinated polyimides (FPIs) that exhibit outstanding optical transparency as well as excellent thermal, mechanical, and electric properties for the applications to optical components, in particular for telecommunication applications. The optical transparency of polyimides in the near-infrared (NIR) region are explained based on the harmonic oscillations of infrared absorptions. The variations and the methods of controlling refractive indices, birefringence, and thermo-optic coefficients of polyimides are described, and a variety of recent applications of FPIs to optical components, such as single-mode and multi-mode waveguide circuits, substrates for WDM filters, waveplates, and polarizers are reviewed. Partially fluorinated and perfluorinated polyimides are promising optical materials for future telecommunication systems.

Keywords / Optical waveguide / Fluorinated polyimide / Optical communication / Optical transparency / Refractive index / Birefringence / Thermooptic effect /

1. Introduction

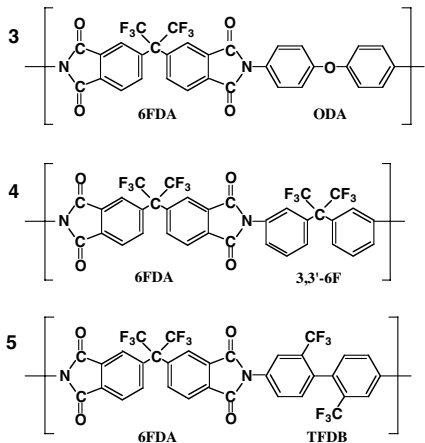
Polyimide (PI) has been recognized as a super-engineering plastic for more than 40 years because of its thermal stability (in general, glass transition temperatures are higher than 250°C, and 5%-decomposition temperatures are higher than 400°C), mechanical toughness, pliability, and outstanding electrical properties (*i.e.* insulation and dielectric properties). Hence, PIs have so far been widely used in the fields of electronics and aerospace applications [1, 2]. In addition, its low dielectric constants and low thermal expansion coefficients are suitable for electronic applications, and its durability against ultraviolet (UV) & visible (VIS) radiation, chemical and environmental resistance are suitable for aerospace applications. On the other hand, researches utilizing PIs as optical materials for telecommunications and optical interconnects made remarkable progress in recent years. These fields require high transparency over the near-infrared (NIR) region, low hygroscopicity, and solder resistance (270–300°C). These properties enable PIs to be hybridized and/or monolithized with semiconductor components for opto-electronics [1a]. However, as seen in the most well-known PI of PMDA/ODA (Kapton, **1**) derived from pyromellitic acid dianhydride (PMDA) and 4,4'-diaminodiphenyl ether (ODA) exhibits strong coloration from yellowish brown to blackish brown, and the absorption edges pulls the skirt to near 550 nm. In addition, the ordering structures at nanolevel deteriorate the transpar-



ency of conventional PIs in the UV, VIS, and NIR regions due to the Rayleigh scattering. In order to utilize PIs as optical materials by overcoming these disadvantages, an introduction of fluorine atoms is a very effective way.

Fluoropolymers exhibit outstanding characteristics, such as low water absorption, low dielectric constants, water and oil repellency, chemical and thermal stability, and fire retardancy, which are well represented by Teflon [3]. However, the decrease in adhesiveness and the very low affinity with other material are frequently troublesome, and the deterioration of solvent-proof nature and mechanical strength (elastic modulus) occur in some cases.

Since any C-H bonds in polymers can be theoretically substituted by C-F bonds, a lot of fluorinated PIs (FPI) have so far been synthesized. In general, fluorination provides unique properties to PIs, such as (I) Reduction of dielectric constants and refractive indices, (II) Improvement of the transparency in the visible and NIR region, (III) Lowering of T_g , (IV)



Change of reactivity of compounds (in particular, decrease in reactivity of diamine), (V) Increase of free volumes, (VI) Decrease of water absorption, (VII) Rise of thermal decomposition temperature, (VIII) Increase in solubility, (IX) Increase of gas permeability, (X) Improvement of radiation-durability, and (XI) Increase of thermal expansion coefficients [4]. The present objectives to develop functional FPI optical materials is to pull out more excellent characteristics without reducing the inherent characteristics of original good nature of PIs.

2. Optical Properties of Fluorinated Polyimides (FPI)

2.1 The FPIs of the First Generation

In 1964, Rogers et al. at DuPont [5] first synthesized a fluorinated polyimide from an acid dianhydride (6FDA) having two benzene rings connected by a hexafluoro-isopropilidene group ($-\text{C}(\text{CF}_3)_2-$: what we call '6F linkage'), and diamine (4,4'-6F) (2). The films obtained were transparent, colorless, and soluble in polar organic solvents. St.Clair et al. at NASA synthesized various kinds of PIs from 6FDA and a variety of diamines containing ether-linkages ($-\text{O}-$). They reported that such PI films exhibit high transparency in the visible region, low dielectric constants, and good solubility to polar organic solvents [6-10]. The wavelengths of absorption edges for PIs derived from 6FDA and diamines having 6F, ether, and sulfone ($-\text{SO}_2-$) linkages are shifted to shorter wavelengths by 100~150 nm than conventional PIs, and thus colorlessness or very pale yellow PIs are obtained. In addition, PIs derived from 6FDA are amorphous and soluble in polar solvent. They serve as typical FPIs due to the good thermal resistance (represented by T_g over 300°C) and the good balance of physical properties. Reuter et al. at IBM [11] reported the optical properties of three kinds of FPIs (2, 3, 4) paying attention as an optical waveguide material for the first time. The FPIs exhibit optical trans-

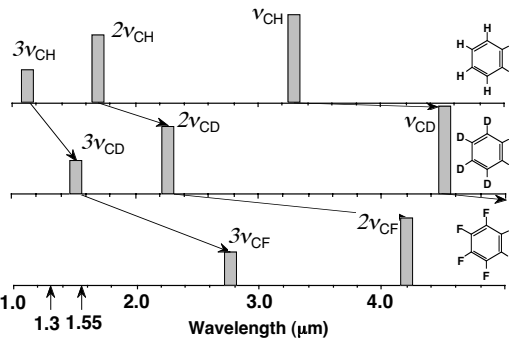


Fig. 1 Fundamental and harmonic absorptions of C_6H_6 , C_6D_6 , and C_6F_6 appearing in NIR and IR regions [18].

mission losses of less than 1/10 of those of nonfluorinated PIs at the wavelength of 0.63 μm . As St.Clair et al. had reported, their absorption edges reflecting their electronic transition absorptions are shifted to shorter wavelengths by 20-50 nm by fluorination. However, when such FPIs are annealed above 300°C, ordering structures are generated, which cause light scattering, and then the optical losses quickly increased ($> 2.5 \text{ dB/cm}$). Feger et al. [12] have reported that the increase in optical transmission losses caused by annealing is decreased at 0.83 μm than at 0.63 μm . On the other hand, Sasaki et al. [13] reported that the optical transmission loss of 6FDA/TFDB (5) (0.16 dB/cm) was maintained after annealing at 350°C for 1h at 1.3 μm . This originates from the higher T_g (ca. 335°C) of the polyimide. Moreover, Wu et al. [14] introduced a small amount of heat-resistant nonlinear dye into 6FDA/TFDB and performed polarization treatments. They reported that little degradation was observed at elevated temperatures.

2.2 Improvement of Optical Transparency

When polymeric materials are used as optical transmission medium in NIR region (wavelengths : 0.85~1.65 μm) such as an optical fiber or optical waveguides in opto-electronic integrated circuits (OEIC), large optical transmission losses generally pose problems. The origin of the losses are 'absorption' and 'scattering'. The wavelengths of light used for optical communications and interconnects have been gradually shifted to longer wavelengths with the progress of technology (from visible light to 0.85 μm , 1.31 μm , and 1.55 μm), and accordingly, the optical losses originating from the infrared oscillating absorptions, which are inherent to the chemical structures of polymers, become dominant. Conventional amorphous polymers, such as PMMA and polystyrene (PS), show good transparency in the visible region, but they exhibit appreciable optical losses in

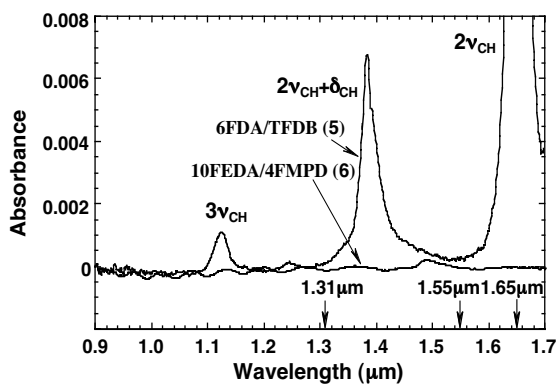
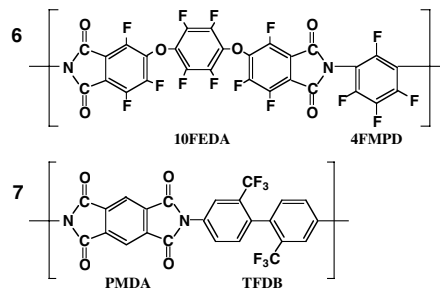


Fig. 2 Absorption spectra of 15 μm -thick films of a partially fluorinated and a perfluorinated polyimide [18].

NIR region. For using polymeric materials as optical transmission medium, the harmonic absorptions resulting from the C–H (and N–H, O–H etc.) bonds should be shifted to longer wavelengths. As a principle, it has been clarified that substitution of deuterium (D) or fluorine (F) for hydrogen is very effective in reducing the optical losses in NIR region, and concrete examinations have been made by replacing hydrogens in PMMA or PS by monovalent heavy atoms, such as deuterium, fluorine, and chlorine [15–17]. Figure 1 shows the effects of substitution by deuterium or fluorine, in which the 2nd and 3rd harmonics of C–H stretching vibrations are significantly shifted to longer wavelengths [18] (the coupling absorptions with bending vibrations are not shown for simplicity). The deuterium substitution is very effective in reducing the loss at 1.3 μm . However, it is inadequate for the reduction in the whole range of optical-communications wavelengths because the 3rd harmonics of C–D bond appears near 1.5 μm .

In contrast to PMMA or PS, the proportion of C–H bonds per unit volume is very low in aromatic PIs because of the absence of alkyl chains. Hence, fluorinated PIs (FPIs) exhibit relatively good optical transparency in NIR region. However, since the strong absorption due to the coupling vibration of O–H bond of absorbed moisture (H_2O) appears at 1.4 μm , hygroscopic polymers like conventional PIs are not suitable for optical use. In contrast, since the absorption of moisture is effectively suppressed by the water repellency of fluorines, and the optical transparency is significantly improved by the reduction of the charge transfer (CT) interactions, FPIs are much suitable for optical uses than conventional PIs. In addition, the numbers of hydrogen atoms per unit volume for FPIs are 1/3 or smaller than those of PMMA or PS, and they include only one kind of hydrogens that are directly bonded to benzene rings. These features reduce the linewidths of absorption peaks. The optical



absorption spectrum of an FPI, 6FDA/TFDB (5), in NIR region is shown in Fig. 2. The absorption peaks that cause optical losses larger than 0.1 dB/cm are the 2nd ($2\nu_{\text{CH}}$; 1.65 μm) and the 3rd harmonics ($3\nu_{\text{CH}}$; 1.15 μm) of aromatic C–H bonds, the coupling vibrations ($2\nu_{\text{CH}}+\delta_{\text{CH}}$; 1.40 μm) of 2 ν_{CH} and the C–H bending vibration, and the 2nd harmonics ($2\nu_{\text{OH}}$; 1.44 μm) of O–H bond resulting from absorbed moisture. Although the optical losses in the 1.55 μm -band are less than 0.1 dB/cm because the wavelengths are located in a ‘absorption window’, but the absorption edges of $2\nu_{\text{CH}}$ and $2\nu_{\text{OH}}$ are slightly overlapped with the 1.3 μm -band. If moisture is completely removed from the preparation process of the films, the absorption originating from $2\nu_{\text{OH}}$ can be eliminated. However, the absorption caused by the skirt (tailing) of $2\nu_{\text{CH}}$ is essential to this material. Since partially fluorinated polyimides contain plural phenyl C–H bonds in the molecular chains, the optical losses caused by the harmonic vibrations and the coupling of the harmonic and the bending vibrations in the range 1.30 ~ 1.55 μm are not negligibly small. Moreover, the wavelength regions that attain low losses are limited to the windows. The polymeric material in the next generation is expected to show very low optical losses in the wide range of NIR, and it is desirable to exhibit no absorption peaks throughout the optical-communications wavelengths.

In 1992, Ando et al. have proposed and synthesized ‘perfluorinated polyimides’ (6) [18–21] for the first time that contain no hydrogen. The optical absorption spectrum is shown in Fig. 2. As expected from the chemical structure, no absorption peaks are observed throughout NIR region except for the absorption near 1.48 μm originating from absorbed water and the 4th harmonic of asymmetrical stretching vibration of imide carbonyl (C=O) group. Excellent optical transparency is attained in the 1.53~1.58 μm region. This material is very promising for future optical communication systems. Since the electron affinity of 10FEDA (the acid dianhydrides used for this PI) is close to that of PMDA, the coloration of prepared film is pale yellow, and the optical transparency in the visible region is inferior to those of par-

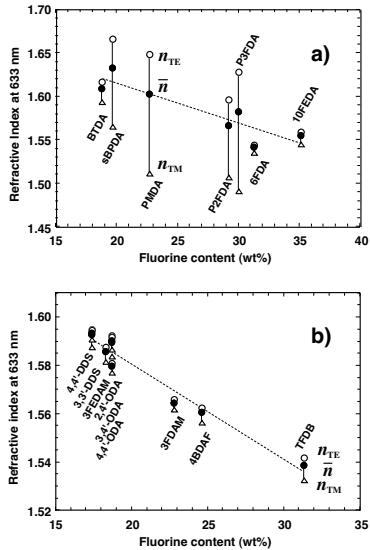


Fig. 3 a) Relationships between the refractive indices (n_{TE} , n_{TM}) and the birefringence (Δn) in case that the diamine is fixed to TFDB, and b) that the dianhydride is fixed to 6FDA [1,22-24].

tionally fluorinated PIs and semi-aromatic PIs.

2.3 Control of Refractive Indices and Birefringence

FPIs are generally amorphous and exhibit high transparency with sufficient thermal resistance. In addition, since their dielectric constants and hygroscopicity are considerably low, they can be used in many applications for optical components. Koshoubu et al. [22-24] investigated the variations in average refractive indices (n_{av}) and birefringence by chemical structure of FPIs (1) in case that the diamine is fixed to TFDB and dianhydrides are changed (Fig. 3a) and (2) that the dianhydride is fixed to 6FDA and diamines are changed (Fig. 3b) (The abbreviations of polyimides used over the figures are to be refer to Ref.1). The n_{av} of PIs decrease linearly with the increase in fluorine content in both cases. Since TFDB has a rod-like structure, the birefringences Δn ($= n_{TE} - n_{TM}$) of PIs exhibit significant changes depending on the anhydride structure. It is in the order of PMDA > P3FDA > sBPDA > P2FDA > BTDA > 10FEDA > 6FDA. On the other hand, as Reuter et al. [11] have clarified, when 6FDA is used as a dianhydride, small values of Δn are always obtained as seen in Fig. 3b, and the correlation with fluorine contents is much better than in Fig. 3a. These results indicate that the control of n_{av} by varying the fluorine content is easier than the control of Δn . The magnitude of Δn is not well correlated with the fluorine content.

Further, Matsuura et al. [25] attempted simultaneous control of n_{TE} , n_{TM} and Δn by copolymeriza-

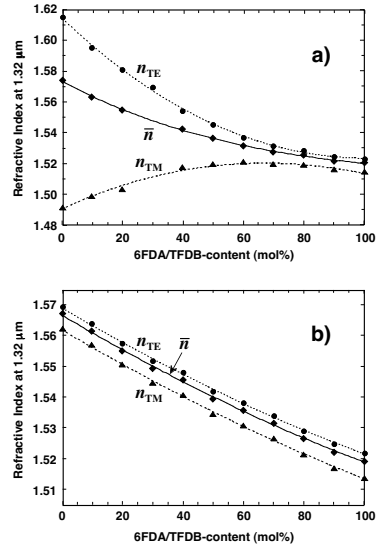


Fig.4 a) Changes in refractive indices (n_{TE} , n_{TM}) for PMDA/TFDB-6FDA/TFDB copolyimide [25], and b) 6FDA/4,4-ODA-6FDA/TFDB copolyimide [27].

tion of two kinds of FPIs (Fig. 4a) with different fluorine contents. The Δn of a spin-coated film of PMDA/TFDB (**7**) is 0.1232, and that of 6FDA/TFDB (**5**) is 0.0082 ($\lambda=1.32 \mu\text{m}$). There is a large difference in Δn between **7** and **5**, and the n_{av} of the copolymers falls rapidly with the increase in the 6FDA content. However, a change of n_{av} by 3.4 % can be achieved by varying the 6FDA content, and the Δn becomes almost stable above the content of 70 %. Succeedingly, Matsuura et al. [26, 27] found that the n_{av} of 6FDA/ODA (**3**) is slightly higher than that of 6FDA/TFDB (**5**) by 3.1 %, and the Δn of the former (0.0072) is almost equivalent to the latter. They synthesized a series of copolymers of **3** and **5** and measured the refractive indices (Fig. 4b). The n_{av} changes linearly to the 6FDA/TFDB content, and moreover, the n_{av} can be precisely controlled with Δn as low as 0.0069~0.0082. Since the Δn is stable with the copolymerization content, refractive-index control on the both sides of TE (electric field is parallel to the film surface) and TM polarizations (electric field is perpendicular to the film surface) becomes easy, and polarization dependent loss (difference of the losses between TE and TM modes) in optical waveguides can be reduced. This is suitable for fabrication of waveguides with arbitrary differences in refractive indices. On the other hand, the Δn of all FPIs synthesized from 10FEDA (**6**) is quite small as 0.004, and the value obtained are in the minimum level of all aromatic polyimides [18-21].

As another technique, Maruo et al. [28] reported that fluorine atoms in FPI (**5**) can be eliminated by irradiation of electron beam. They found that the

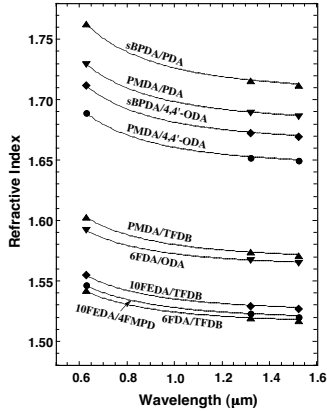


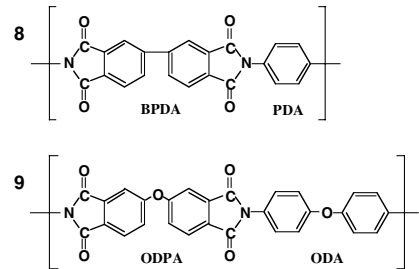
Fig. 5 Wavelength dispersion of the average refractive indices of polyimides [30].

refractive index of an irradiated part increases in proportion to the total dose of irradiation, and thus the refractive index can be precisely controlled. By using focused electron beam, optical waveguides can be directly drawn on FPI thin films.

Moreover, Yoshida et al. [29] prepared a novel FPI system, in which TiO_2 nano-particles having a higher refractive index are dispersed, and succeeded in controlling the n_{av} from 1.550 to 1.560 at 0.63 μm . By making TiO_2 particle into nanometer size (with a volume concentration of particle of 4 wt%), the light scattering is well controlled, and the optical propagation loss for the FPI- TiO_2 hybrid material was reported as 1.4 dB/cm

2.4 Wavelength Dispersion of Refractive Indices

Abbe number is commonly used for estimating wavelength dependence (dispersion) of refractive indices of optical material. However, this is not suitable to estimate the dispersion at longer wavelengths in the visible region and the NIR region for aromatic PIs. Since conventional PIs exhibit absorption edges



at 0.4~0.55 μm , and the anomalous dispersion arises near the absorption edges. Ando et al. [30] reported the dispersion of nine kinds of PIs. Average refractive indices (n_{av}) were measured at three wavelengths of 0.633, 1.312, and 1.523 μm ($n_{0.633}$, $n_{1.312}$, and $n_{1.523}$) and the fitted curves using the simplified Cauchy formula were presented (Fig. 5). The refractive index at the infinite wavelength (n_∞) is linearly proportional to the coefficient of wavelength dispersion C , which indicates that PIs having higher refractive indices exhibit large dispersion. By using the obtained fitted formula, it makes possible to predict $n_{1.312}$, $n_{1.523}$, and n_∞ from $n_{0.633}$ for most of PIs.

2.5 Control of Thermo-Optic Coefficients

Strong attentions have been paid to the temperature dependence of refractive index of polymers formed on substrates. This phenomenon, that a refractive index decreases with the temperature increases, is called thermo-optic (TO) effect. In the optical waveguides field, this effect can be used for fabrications of optical controlling circuit, such as digital TO switch, Mach-Zehnder TO switch, variable attenuator, and optical circuits widely used for temperature compensation circuits etc. Since these circuits are fabricated on substrates such as silicon (Si), the method for evaluating TO coefficient (dn/dT) of films is required the control of polarization of incident light. In particular, the evaluation of polarization dependence is important for the design of circuits, but the TO coefficients reported for optical polymers are limited to bulk samples. Kobayashi et al. [31] fabricated several waveguide circuits using FPIs. A value of $dn/dT = -150$ ppm/K was obtained from the temperature displacements of the wavelength of a certain output of AWG (see below). Very recently, Terui et al. [32, 33] measured TO coefficients for 7 kinds of aromatic PI films (1, 3, 5, 6, 7, 8, and 9) formed on Si substrates using the prism coupling method (Fig. 6), in which the temperature was precisely controlled using three sets of ceramic heaters. Isotropic (average) values (dn_{av}/dT) are in the range $-59 \sim -94$ ppm/K, and the dn_{av}/dT increases as the n_{av} increases except for a semi-crystalline PI (8). For

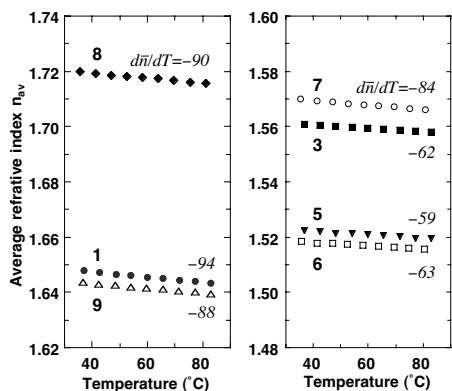


Fig. 6 Temperature dependence of the refractive indices of polyimides (TO coefficients [ppm/K]) [32,33].

all PI films, the absolute values of dn_{TE}/dT are larger than dn_{TM}/dT , indicating remarkable anisotropy ($dn_{TE}/dT - dn_{TM}/dT$) in the TO coefficients in the range of $-9 \sim -39$ ppm/K. These anisotropy is not closely related to the degrees of refractive index or birefringence. This phenomenon may cause significant polarization dependence in the performance of TO switches, but this can also be used for polarization-sensitive optical filters or splitters etc.

3 Applications of FPIs to Optical Use [34]

3.1 Thin FPI-Film Substrates for Multilayer Filters

Flexible substrates for supporting “thin film filters” is a good example of the applications of outstanding optical transparency of FPI over the visible and NIR regions with good heat resistance, pliability, and good processability as thin films. For optical communication applications, optical filters have a function that they are transparent for specific wavelengths but reflective for other wavelengths. An optical filter consists of a dielectric multilayer, which performs transmission/reflection of light, and it is formed on a supporting substrate film. It is strongly required that the thickness of a filter inserted into optical circuits, such as an optical fiber or optical waveguides, should be less than 20 μm in order to reduce the radiation loss accompanying with a groove formed in the optical circuits. For conventional bulk-type filters, multilayered thin film of TiO_2 and SiO_2 is formed on an inorganic glass or silica substrate by sputtering, in which the cost for making thin film and grinding and polishing the substrate is rather high. On the other hand, since formation of FPI thin films is easy and economical by spin-coating [35], and the optical transparency and heat resistance is excellent, FPI is the best material for substrates of multilayer filters. Paying attention to the suitable properties of an FPI 7, thin film filters were fabricated using this PI as a substrate. Optical filters having a function of 1.3 μm -transmission / 1.55 μm -reflection were produced using inorganic glass and FPI substrates, and almost the same properties were obtained. At present, thin PI film filters are produced and widely used in the WDM modules for optical surveillance systems in fiber-optics communications.

3.2 Thin FPI-Film Waveplates

“Thin film polyimide waveplate” is a good example of application using the large birefringence nature of FPIs having rigid-rod molecular structures with outstanding optical transparency. Silica-based planar lightwave circuits (PLCs) formed on Si substrates are widely used for optical communications because

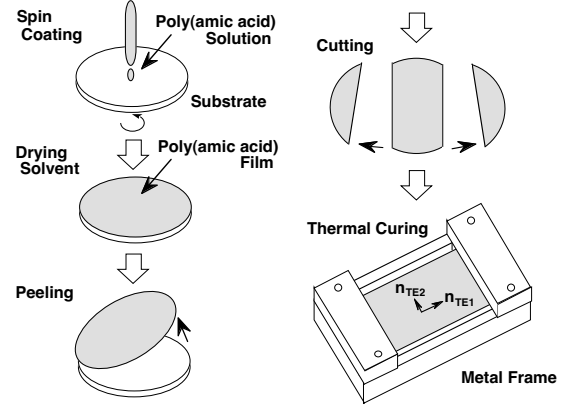


Fig. 7 Method of preparing polyimide waveplate using the spontaneous orientation behavior [37-40].

of their high performance and mass-productivity. However, the optical components using interference of light frequently show apparent polarization dependence resulting from the birefringence of optical waveguides, and this had been a serious problem [36]. As a technique for solving this, the polarization mode exchanging method which inserts a half-waveplate at the center of optical path of PLC was proposed. However, when using a conventional half-waveplate made by quartz (92 μm -thick), excess insertion loss (radiation loss) is more than 5 dB due to the large thickness. In order to reduce the loss, the thickness of a waveplate should be reduced, and thus, it is necessary to produce a waveplate using highly birefringent materials. Moreover, ease at insertion, outstanding optical transparency at the operating wavelength, and high reliability over high temperature and high humidity are required as same as for optical filters. Ando et al. [37-40] focused on the rigid-rod molecule structure of a FPI 7. Although PI thin films can be easily formed by spin-coating of polyamic acid solution (precursor) on a substrate followed by heating, the films thus produced is optically isotropic in the film plane. Hence, no in-plane birefringence ($\Delta n_{//} = \Delta n_{TE1} - \Delta n_{TE2}$) is generated. Then, spin-coated polyamic acid solution was partially dried at a low temperature, and peeled from the substrate. The film was fixed to a metal frame by two sides of the longer direction. The PI molecules are spontaneously orientated along the fixed direction during thermal imidization at 350°C, and thus large birefringence ($\Delta n_{//} = 0.053$) was generated in the film plane. (Fig. 7). The magnitude of birefringence is controllable with high precision by changing the curing conditions, in particular the highest imidization temperature. A PI waveplate exhibiting a large Δn (0.18), that is 20 times larger than quartz, is producible by using this technique. As a result, the thickness of a novel PI waveplate of 14.5 μm for a

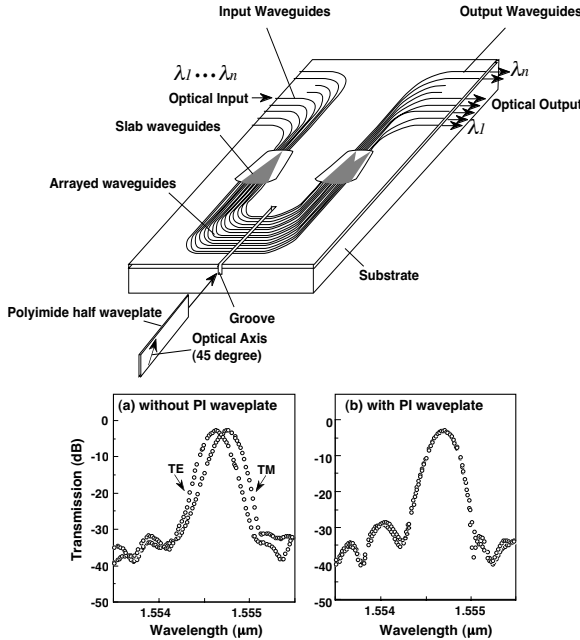


Fig. 8 Insertion of a thin polyimide waveplate into a groove formed in an arrayed waveguide grating (AWG) (top), and the effect of elimination of polarization dependence by the PI waveplate (bottom) [31].

wavelength of $1.55\text{ }\mu\text{m}$ is about $1/6$ of conventional quartz waveplate. Accordingly, the resulting drastic decrease in the thickness of half-waveplate also sharply reduced the insertion loss to less than 0.3 dB . Furthermore, since it has outstanding heat resistance (350°C) and good pliability, PI waveplates contributed to the improvement in reliability and low costs of optical components. Matsuda et al. [41, 42] clarified that the intrinsic birefringence (the birefringence when all polymer chains are uniaxially orientated in one-direction) of PIs having rigid structures ($0.33\text{--}0.51$) can far exceed the values of calcite (0.172) and rutile (titanium dioxide : 0.287). Further applications of the highly birefringent nature of uniaxially drawn FPIs to optical components are expected.

An example of application of a PI half-waveplate to arrayed waveguides multiplexer (AWG) is shown in Fig. 8. A waveplate is inserted into a thin groove formed at the center of lightpath of the AWG circuit and is being fixed with optical adhesive. The peak wavelengths of optical output differ between the TE and TM polarizations after wavelength separation due to the intrinsic birefringence of the optical waveguides. However, by inserting a PI waveplate, the peak wavelengths of the AWG coincide for TE and TM polarizations, and thus the polarization dependence of the whole circuit was eliminated. The excess loss of the waveplate was estimated as 0.26 dB , which is $1/15$ or less than the loss with a quartz waveplate [38]. Moreover, the degree of polariza-

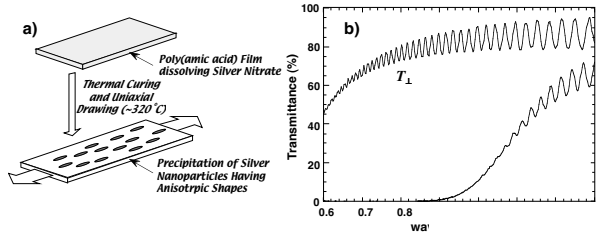


Fig. 9 a) Preparation of silver nanoparticle dispersed and uniaxially drawn polyimide film and b) polarized transmission spectra of the films obtained [44-46].

tion conversion of a FPI waveplates is more than 25 dB and the amount of reflective attenuation is below -30 dB [39]. These performance suffices the demands for dense WDM systems that will be introduced in the near future.

Since the FPI waveplates are very effective in eliminating the polarization dependence of interfered-type lightwave circuits, they can also be used for directional couplers, asymmetrical Mach-Zehnder interferometer-type wavelength multiplexers, optical branching circuits, and wavelength dispersion equalizers. Moreover, Sawada et al. [43] have fabricated a ultrathin film reflective-type FPI waveplate with a thickness of $5\text{ }\mu\text{m}$. A $0.1\text{ }\mu\text{m}$ -thick gold film was formed on a FPI waveplate by sputtering, and then the hybrid film functions as a reflective waveplate. LiNbO_3 is fragile as optical waveguide material, and it is very difficult to form a thin glove. A PI reflective waveplate was attached at the end of waveguides, and thus the polarization dependence was completely eliminated, and miniaturization of components and switching at a low voltage were attained.

3.3 Thin FPI-Film Polarizers

By using FPI films that exhibit excellent optical transparency and pliability, optical components can be fabricated by small sizes. Polarizer is a fundamental optical component that transmits only a specific linear polarization. Conventionally, thin film polarizers have been fabricated by uniaxially drawn inorganic glass containing ultrafine- or nano-particles of metals (silver and copper). Ando et al. [44] dissolved silver nitrate in a polyamide acid (PAA) solution of 7 , and formed a PAA film followed by uniaxial drawing during thermal curing. They found out that silver nanoparticles having a long and slender form (whisker shape) were precipitated and deposited in the films after imidization. The precipitation of silver nanoparticles having anisotropic shapes were promoted by the high degree of orientation of polyimide chain that is well reflected to the large birefringence of FPIs. The uniaxially drawn FPIs function well as

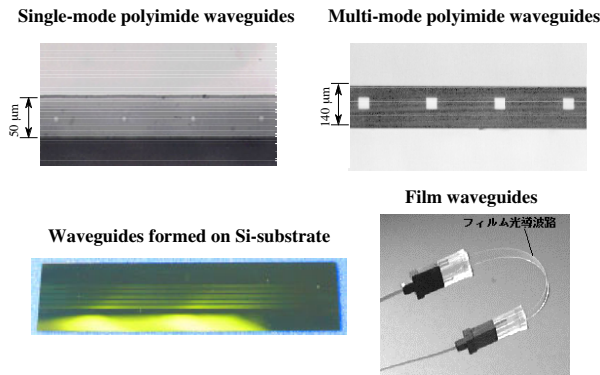


Fig. 10 A variety of polyimide waveguides (the diameters of the cores for the single and multi-mode waveguides are 8 and 50 μm , respectively).

very transparent but highly anisotropic media. Since the fundamental absorption wavelength of the plasmon resonance absorption of Ag nanoparticles differs greatly in the directions parallel and perpendicular to the elongation direction, the high polarization characteristic (larger dichroic ratios) can be achieved in the visible and NIR regions. Recently, Matsuda et al. [45, 46] optimized the heat treatment conditions and the atmosphere of imidization, and produced thin film (14.5 μm -thick) FPI polarizers whose extinction ratios are larger than 25 dB (500:1) at a wavelength of 0.85 μm (Fig. 9).

3.4 Planar Optical Waveguides of FPIs

Optical waveguide is a fundamental component which confines an optical signal in a specific domain, and the light propagates from the incident edge to the other edge. The domain having a high refractive index is called ‘core’ which are surrounded by a domain having a lower refractive index called ‘cladding’. Waveguides can be roughly divided into two groups, “planar (slab) waveguides” and “channel waveguides”. The former has a spread waveguides at two dimensions. In the latter, light propagates in one dimension due to the confinement of light in their cores.

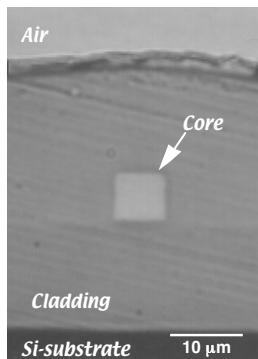


Fig. 11a The cross-sectional view of the core of a single-mode FPI waveguide [51,52,54].

The idea to use PIs for optical waveguide materials is not new. In 1982, Furuya [47] at the Bell Lab of AT&T fabricated a semiconductor laser with slab waveguides using conventional polyimides (DuPont Pyralin PI-2555). The structure of waveguides were prepared by two cladding layers with a low refractive index in the upper and lower sides of a planar waveguide (core layer), in which light was confined in the vertical direction. The propagation loss of this optical waveguides was reported as 3 dB/cm at a wavelength of 0.5 μm . After that, various kinds of PI optical waveguides have been fabricated and examined for the purpose of optical interconnection in optoelectronic integrated circuits (OEIC). Since most of the researches have been in the electronics field, conventional PIs that have been used for insulator and aerospace applications were used for waveguide fabrications, but a few chemists tried to develop novel polyimides which are suitable for optical uses. In 1993, Kowalczyk et al. [48] produced planar slab waveguides using a photosensitive FPI (Amoco Ultradel 9020D) formed on a thermally oxidized Si wafer. They reported that the optical loss was 0.4 dB/cm in actual measurement at the wavelength of 0.8 μm and 0.3 dB/cm as a predicted value at 1.3 μm . Moreover, Franke et al. [49] fabricated planar waveguides using two kinds of FPIs : 6FDA/4-4'-6F (2) and 6FDA/3,3'-6F (4). They aimed to apply the waveguides to humidity sensor utilizing the good sensitivity of the propagation characters of PI waveguides to humidity.

3.4.1 Channel-Type Optical Waveguides

In recent years, planar optical waveguides components including planar lightwave circuits for optical wiring and interconnections have been fabricated using technologies for fine patterning and processing of PI thin films formed on substrates. In addition, a

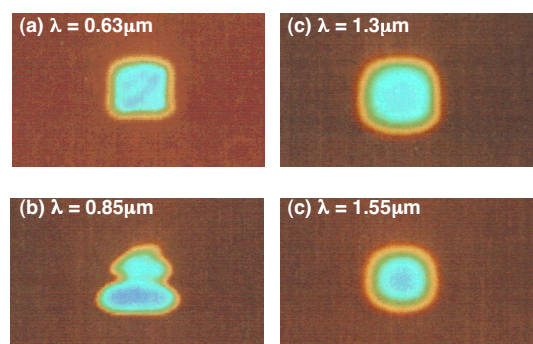


Fig. 11b The optical power distribution (near field patterns) of a polyimide waveguide measured at different wavelengths. Single-mode operation is attained at 1.3 and 1.55 μm [51,52,54].

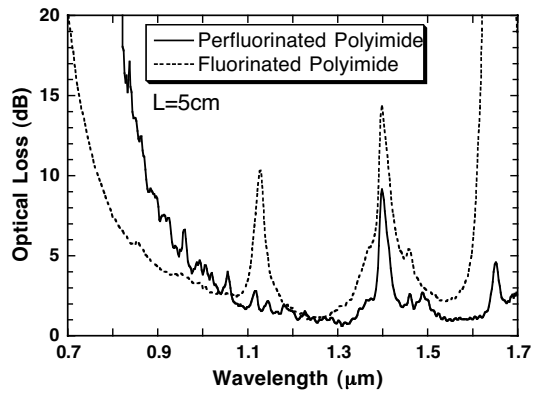
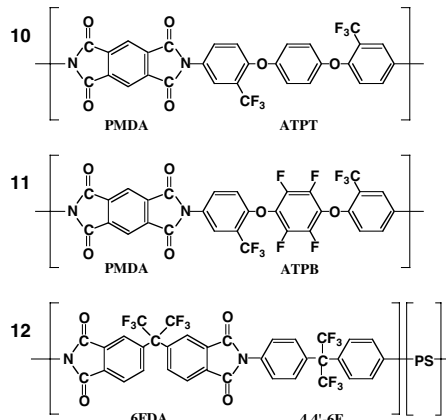


Fig. 12 Optical loss spectra of single-mode waveguides prepared by perfluorinated polyimide and partially fluorinated polyimide [58].

variety of optical circuits combining straight lines, curves, branches, and intersections have been reported. These optical wirings are composed of “channel-type optical waveguides” that can be divided roughly into “ridge-type optical waveguides” in which the core is exposed, and “embedded-type optical waveguides” in which the core is embedded by sheath material (cladding). For advanced optical circuits and interconnects, only the embedded-type can be used because these require the single-mode operation.

3.4.2 Waveguides Fabricated by Dry-Etching

In 1988, Sullivan et al. [50] formed PI thin films that were specially developed for optical use on a thermally oxidized Si substrate, and produced a 1x4 branch-type lightwave circuits, and an 8x8 optical matrix circuit using silicone oxide and two-layer mask of photoresist. At a wavelength of 0.83 μm , the propagation loss of 0.15 dB was reported for a straight line, and 0.4 dB for a 45° bent. In addition, the optical losses of these circuits were 0.03 dB for a 1x2 branch, 0.3 dB/cm for an intersection, and 0.4 dB for a 90° bent. Considering their multi-mode operation, the losses were surprisingly low. Matsuura et al. [51] produced ridge-type PI waveguides using copolymers of **5** and **7** on thermally oxidized Si substrates. Both FPIs exhibit excellent optical transparency at the optical communication wavelengths in NIR region. They reported the propagation loss for a straight line was 0.3 dB/cm, and the connection loss with a silica fiber was 0.5 dB at 1.3 μm . Moreover, they fabricated embedded-type optical waveguides for the single-mode and multi-mode operations using copolymers of **5** and **7** whose refractive indices were precisely controlled by varying the copolymerization ratio [52] (Fig. 10). The magnified core of an embedded-type single mode waveguide and the power distributions of the optical output on the facet (near-field patterns) of the optical waveguides are shown in

Fig. 11. The operation is multi-mode at the wavelengths of $0.63\text{ }\mu\text{m}$ and $0.85\text{ }\mu\text{m}$, in which the spreading optical power is distributed in complicated ways. However, typical Gaussian distributions are observed at the center of the cores with the strongest power distribution at the wavelengths of 1.3 and $1.55\text{ }\mu\text{m}$, which indicates the single-mode operation. The propagation loss of this single-mode optical waveguides was 0.27 dB/cm at $1.3\text{ }\mu\text{m}$, and the connection loss with a single-mode optical fiber was 0.25 dB .

Since FPIs exhibit outstanding heat resistance and low water absorptivity, optical waveguides fabricated using FPIs are also excellent in thermal stability of optical loss and moisture resistance. Kobayashi et al. [53] evaluated the heat and moisture resistance of single mode embedded-type waveguides produced by copolymers of **3** and **5**. The optical losses did not change after annealing at 380°C for 1h and after keeping at a relative humidity of 85 % at 85°C for 200 h.

The above mentioned FPI optical waveguides are usually fabricated on Si substrates like silica-based PLCs. However, they can also be used as self-standing film-type waveguides by removing substrates because of the pliability of FPIs (Fig. 10). The residual stress originating from the mismatch of thermal expansion with the substrate can be released by additional annealing. The polarization dependent loss and the birefringence can also be reduced by annealing. The propagation loss of FPI film waveguides was reported as 0.3 dB/cm at 1.3 μ m, and the polarization dependent loss was below 0.1 dB/cm. Moreover, the measured birefringence (Δn) is almost equivalent to silica-based optical waveguides. The value of 9×10^{-5} for Δn is 1/100 or less than those of FPI waveguides formed on Si substrates [54].

As an example of application of optical waveguides

using FPIs with different molecule structures, Kim et al. [55] formed a thin film by UV irradiation and heat treatment using photo-curable FPIs, and they tried to fabricate channel-type optical waveguides by ICP (Inductively Coupled Plasma) etching of oxygen using a SiO_2 mask. Moreover, Han et al. [56] synthesized copolymer of FPIs with different fluorine contents (**10** and **11**), and they fabricated embedded-type optical waveguides. The refractive index control range of this copolymer is 1.5397 to 1.5671 at 1.55 μm for the TE mode, and a difference in refractive indices of 1.7% was attained. The propagation loss for the embedded-type optical waveguides (core depth and width were 1.6 μm and 6 μm , respectively) was below 0.5 dB/cm at 1.55 μm . On the other hand, Han et al. [57] synthesized copolymer of **3** and fluorine- and chlorine-containing PIs, and fabricated embedded-type waveguides. The refractive indices of PIs increase with the increase in the chlorine content, and they can be controlled within 3.4 % from 1.5176 to 1.5714 in the TE mode at 1.55 μm . The propagation loss of the embedded-type waveguides fabricated from this material was below 0.4 dB/cm and the polarization dependence loss was below 0.1 dB/cm at 1.55 μm .

Since a perfluorinated PI (**6**) show no absorption peaks in NIR region, very high transparency is expected both at 1.31 and 1.55 μm , which is very advantageous as a waveguide material. Very recently, Kagei et al. [58] fabricated embedded-type waveguides using perfluorinated PIs for the core and cladding, and the single mode operation was confirmed. The propagation losses were 0.10 dB/cm for TE mode and 0.18 dB/cm for TM mode. As shown in Fig. 12, no absorption peaks are observed throughout NIR region except for the absorption peak at 1.39 μm which is attributable to the 2nd harmonics of stretching vibration of O-H of water absorbed in the waveguides and/or the 4 th harmonics of the asymmetrical vibration of imide C=O.

3.4.3 Channel Waveguides by Photosensitive FPIs

The above-mentioned channel-type FPI waveguides have been fabricated by fine patterning and processing by reactive ion etching (RIE) technique using oxygen gas with lithography using photoresists. On the other hand, photo-sensitive molecules can be mixed or photo-sensitive moieties can be introduced into the main chain or side chain structures of FPIs. This means that channel-type waveguide can be easily fabricated by exposure and development of FPIs without RIE processes. Beuhler et al. [59] fabricated channel-type waveguides using FPIs, in which photo-sensitive cross-linkable moiety

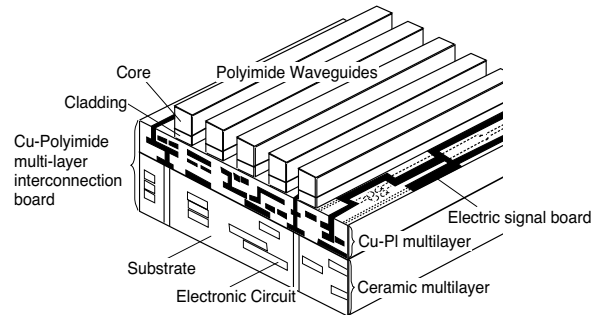


Fig. 13 An example of opto-electronic multi-chip module (OE-MCM) [63].

was incorporated in the the main chain by copolymerization with FPI (**12**). In this material system, the refractive index control of the core and cladding was attained by substituting fluorinated groups with alkyl groups. The propagation loss of the fabricated embedded-type waveguides was below 1 dB/cm at 1.55 μm .

3.4.4 Channel Waveguides by Electron Beam

As mentioned in Section 2.3, when electron beam is irradiated to a FPI (**5**), the refractive index increases due to the elimination of fluorine atoms without loosing the good transparency. Using this phenomenon, Maruo et al. [60, 61] irradiated electron beam on a core layer of FPI thin film, and produced channel-type waveguides. Unlike to the waveguides fabricated by other methods, the core produced by electron beam exhibits specific refractive-index distribution originating from the diffusion and absorption of high-energy electrons to the PI thin layer.

3.4.5 Channel Waveguides by Embossing

For producing channel-type FPI waveguides economically and in large quantities, several methods using metallic molds, stamps, or polymeric transfer molds are proposed. Shiota et al. [62] examined a method to fabricate FPI waveguides using a transfer mold made of PI. The exfoliation layer of SiO_2 was deposited on a FPI transfer mold in advance, and a precursor solution of FPI (copolymer of **3** and **5**) was spin-coated on it, and then a cladding film having trenches that can be used for cores was obtained. Film-type optical waveguides were prepared by spin-coating and following thermal imidization of the core and upper cladding. The propagation loss of the embedded-type waveguides fabricated by this method was 0.3 dB/cm

3.5 Applications of FPI Waveguides to Optical Interconnections

The connection technology between optical fibers

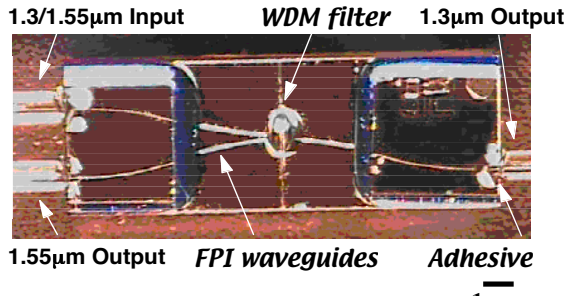


Fig.14 1x2 wavelength division multiplexer [68].

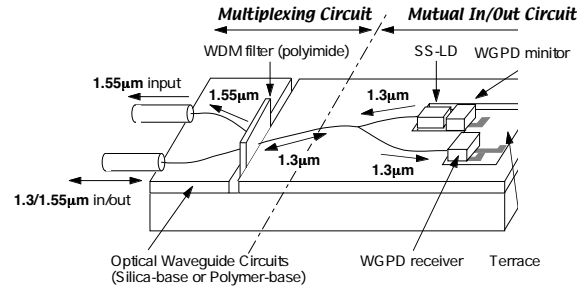


Fig.15 An architecture of Optical Network-ing Unit (ONU) installed in subscribers.

and opto-electronic components for modules in which LSI chips for signal processing are mounted (OEIC) is very important as an application of optical waveguides. Shimokawa et al. [63] fabricated multi-mode ridge-type optical waveguides using FPI copolymers on a multilayer electronic wiring substrate (copper-PIs and ceramics-PIs wiring boards) in 1993. They tried to produce an opto-electronic mixed-loading opto-electronic multi-chip module (OE-MCM) (Fig. 13). The propagation loss of the multi mode waveguides was 0.4 dB/cm at the wavelength of 1.3 μm . Since the diameter of the cores for multi-mode waveguides is as large as 50 μm , deep etching technology was needed for the precise processing of waveguides. It was achieved by RIE technique using oxygen plasma and a titanium mask for a high selection ratio. Moreover, Koike et al. [64] produced a 45° mirror to facet of optical waveguides by leaning the above-mentioned ridge-type optical waveguides by 45° during perpendicular etching. Using optical waveguides with a 45° mirror, vertical surface-type photodetectors (PD) and vertical-cavity surface-emitting laser (VCSEL) can be directly mounted on the surface of waveguide circuits.

3.6 Optical Circuits of FPI Waveguides

Optical waveguides is not only used for simple optical interconnections between module and chips but can form various types of functional components by designing optical circuits. Kobayashi et al. [65] fabricated various types of bent waveguides using copolymers of FPI **3** and **5** on Si substrates with varying the curvature radius. They showed that the minimum bent radius (the minimum curvature for confining light in the core) can be minimized by increasing the difference in refractive indices between the core and cladding. Ukechi [66] examined optical losses in basic waveguide components, such as a straight line, S-curve, and Y-branch, and confirmed validity of application of FPI waveguides to hybrid optical integrated circuits.

3.6.1 Directional Couplers

By combining waveguides of bent structures and straight lines, a directional coupler, a fundamental optical circuit component, was produced by Kobayashi et al. using copolymers of FPI **3** and **5** [67]. Mutual interference of propagating signals is generated at the joint part, at which two optical waveguides adjoined, and the optical output for the through port and the crossing port can be changed by controlling the interval and interaction length of the joint part. A directional coupler whose separation ratio is set to 1:1 is called a 3 dB coupler, and it is a typical 1x2 optical branch component.

3.6.2 Wavelength-Division Multiplexers (WDM)

Katada et al. [68] produced a filter-insertion-type 1x2 two-wavelength division (1.3/1.55 μm) multiplexer (WDM) by combining a thin PI film multilayer filter and Y-branch waveguides fabricated using copolymers of **3** and **5** (Fig. 14). The insertion loss of this WDM was below 3 dB, and the cross talk was below -30 dB. Moreover, Kagei et al. [69] produced a coarse-WDM (CWDM) with four channels by combining three steps of the above-mentioned wavelength multiplexing circuit on one chip. Furthermore, arrayed waveguide grating (AWG)-type WDM is a well known PLC for dense wavelength multiplexing. Since the interference of light occurring in combined array waveguides and slab waveguides are used in AWG, very precise waveguide processing and control of refractive indices are required. Kobayashi et al. [70] succeeded in fabricating a 16-channel AWG using the same FPI copolymers used for the 4-channel CWDM mentioned above.

3.6.3 Digital Thermo-optic Switches

Optical waveguide components using FPIs have been examined for the purpose of improvement in the economic efficiency by using the outstanding processability, good pliability, shock stability, and tractability of PI. Since the temperature dependence

(dn/dT) of refractive indices of polymeric materials including PIs is much larger than silica, thermo-optic (TO) switch can be a good target of polymer waveguide circuits. Kobayashi et al. [71] installed a metal heater on the both sides of a Y-branched waveguide fabricated using copolymers of **3** and **5**, and examined its digital TO switching performance. By using a FPI exhibiting a large TO coefficient, the required electric power for switching can be effectively reduced. Moreover, Ido et al. [72] produced a 1x8 digital TO switch by combining three steps of 1x2 TO switches fabricated by FPIs. On the other hand, Fujita et al. [73] produced a 2x2 TO switch using FPIs by combining a TO switch and an optical attenuator. This circuit can be useful as an add-drop circuit in the WDM systems.

3.6.4 Polarization Splitters

As stated in Section 2.3, aromatic PIs having rigid molecular structures exhibit large birefringence compared with quartz or other organic polymers. Using this character, Oh et al. [74] fabricated a Y-branch optical waveguides by combining waveguides of non-birefringent polymeric materials (polyetherketone, perfluorocyclobutane) and highly birefringent FPIs. For a branch circuit of one side including PI waveguide (TE-branch), the light propagating condition is attained only for the TE mode. Hence, this circuit functions as a polarization splitter which divides the incidence light into the TE polarization and the TM polarization. The insertion loss of this splitter including the connection loss between the waveguides and the input / output-fibers was 3.8 dB at 1.55 μ m, and the cross talk was below –20 dB.

3.6.5 Optical Networking Unit (ONU)

With the progress of optical-communication technology and the Internet technology, the Fiber To The Home (FTTH) projects was started in the last decade. This project aims to introduce optical-fiber networks to every places of working offices and homes in Japan. An opto-electronic mixed-loading components (Optical Networking Unit, ONU, Fig. 15), which perform transmission and detection of optical signals and inter-conversion of optical and electric signals, are indispensable at all subscribers in the FTTH system. Ido et al. [72, 75] produced optical transceiver modules using FPI waveguides at a low cost, and reported that good fundamental properties (optical output > 2mW @ 60mA, detection sensitivity >0.39 A/W) were obtained. Moreover, since the refractive index of the cladding of FPI is higher than that of silica, many advantages are given. For example, the cladding layer of FPI can be thin because the waveguides are fabri-

cated on Si substrate covered by SiO_2 thin layer, and the alignment between the core of waveguide and the semiconductor optical elements (LD, PD) in the vertical direction becomes easy.

4. Summary and Future Prospects

In this article, the outline and circumstances on the basic optical properties and the applications of FPI optical materials are widely reviewed, in particular for aiming at the application to optical components, opto-electronic devices, and optical interconnection. The optical transparency in the visible and NIR regions was greatly improved by partial fluorination of polyimides, but much further progress in the optical transparency at the optical-communications wavelengths was attained by the development of perfluorinated polyimides. The controls in refractive indices, birefringence, and thermo-optic coefficients were also attained by the progress in advanced molecular design, copolymerization, and uniaxial drawing technology. Moreover, the progress in the fine-patterning and processing technology using various methods supports the fine processing of optical waveguides with high precision. Many optical components and optical devices have been already developed, and optical applications of FPIs on the basis of such components are coming to extensive use in near future. Although further examinations are required for the reliability and the optical mounting technology, FPI optical material is promising due to its very attractive characteristics. More active researches are expected to be continued for further progress.

Acknowledgements

The author thanks Dr. F. Yamamoto, Dr. S. Sasaki, Dr. T. Matsuura, Dr. Y. Inoue, Mr. T. Sawada, Mr. S. Matsuda, and Mr. Y. Terui for their helpful discussions and fruitful collaborations.

References

- 1) Y Imai, R. Yokota, Eds. “*Novel Polyimide - Basics and Applications*”, (Japanese) Japan Polyimide Conference, NTS, p.601 (2002).
- a) S. Ando, “*Chemical Structures and Optical Properties of Polyimides*” (Basics Part, Chap.5),
- b) S. Ando, T. Matsuuta, “*Fluorinated Polyimides*” (Application Part, Chap.4).
- 2) Y. Imai, M. Kakimoto, R. Yokota, Eds. “*The Latest Progress in Polyimides, Annual Reports of Japan Polyimide Conference*”, (Japanese) Japan Polyimide Conference, Vol.1 (1993)~ Vol.12 (2004).
- 3) K. Ihara, S. Kojiya “*Fluoropolymers*”, (Japanese) Polymeric New Materials Series-23, Kyoritsu Publisher (1990).

4) G. Hougham, P. E. Cassidy, K. Johns, and T. Davidson, eds. "Fluoropolymers 1: Synthesis" and "Fluoropolymers 2: Properties", Kluwer Academic/Plenum Publishers, New York (1999).

5) F. E. Rogers, U.S. Patent 3,356,648 (1964).

6) A. K. St.Clair, T. L. St.Clair, W. S. Slemp, and K. S. Ezzel, *Proc. 2nd Int. Conf. Polyimides*, Ellenville, NY, p.333-334 (1985).

7) A. K. St.Clair and T. L. St.Clair, *ACS Polym. Mater. Sci. Eng.*, **51**, 62-66 (1984).

8) A. K. St.Clair and W. S. Slemp, *SAMPE J.*, **21**, 28-33 (1985).

9) A. K. St.Clair and T. L. St.Clair, *ACS Polym. Mater. Sci. Eng.*, **55**, 396-400 (1986).

10) A. K. St.Clair, T. L. St.Clair, and W. P. Winfree, *ACS Polym. Mater. Sci. Eng.*, **59**, 28-32 (1988).

11) R. Reuter, H. Franke, and C. Feger, *Applied Optics*, **27**(21), 4565-4571 (1988).

12) C. Feger, S. Perutz, and R. Reuter, *ANTEC'91*, 1594-1597 (1991).

13) S. Sasaki, S. Ando, T. Matsuura, Y. Hirata, F. Yamamoto, *Polymer Prep. Jpn.*, **41**(7), 2845-2847 (1992).

14) M. H. Wu, S. Yamada, R. F. Shi, Y. M. Cai, and A. F. Garito, *ACS Polym. Prep.*, **35**(2), 103-106 (1994).

15) T. Kaino, M. Fujiki, and S. Nara, *J. Appl. Phys.*, **52**, 7061-7063 (1981).

16) T. Kaino, K. Jinguiji, and S. Nara, *Appl. Phys. Lett.*, **42**, 567-569 (1983).

17) T. Kaino, *Appl. Phys. Lett.*, **48**, 757-758 (1986).

18) S. Ando, T. Matsuura, and S. Sasaki, *CHEMTECH*, p.20-27, December (1994).

19) S. Ando, T. Matsuura, and S. Sasaki, *Macromolecules*, **25**, 5858-5890 (1992).

20) S. Ando, T. Matsuura, and S. Sasaki, in "Polymers for Microelectronics, Resists and Dielectrics", L. F. Thompson, C. G. Willson, and S. Tagawa, eds., *ACS Symp. Ser.*, **537**, pp.304-322, American Chemical Society (1994).

21) S. Ando, T. Matsuura, and S. Sasaki, "Fluoropolymers 2: Properties", Chap.14, G. Hougham, P. E. Cassidy, K. Johns, and T. Davidson, eds., Kluwer Academic/Plenum Publishers, New York (1999).

22) N. Koshoubu, T. Matsuura, T. Maruno, S. Sasaki, *Polymer Prep. Jpn.*, **44**, 316 (1995).

23) N. Koshoubu, T. Matsuura, *Polymer Prep. Jpn.*, **44**, 1521 (1995).

24) N. Koshoubu, T. Matsuura, T. Maruno, S. Sasaki, *Polymer Prep. Jpn.*, **45**, 2305 (1995).

25) T. Matsuura, S. Ando, S. Sasaki, and F. Yamamoto, *Macromolecules*, **27**, 6665-6670 (1994).

26) T. Matsuura, N. Koshoubu, T. Maruno, S. Sasaki, *Polymer Prep. Jpn.*, **46**, 662 (1997).

27) J. Kobayashi, T. Matsuura, Y. Hida, S. Sasaki, and T. Maruno, *IEEE J. Lightwave Technol.*, **16**, 1024-1029 (1998).

28) Y. Y. Maruo and S. Sasaki, T. Tamamura, *J. Vac. Sci. Technol. A*, **13**, 2758-2763 (1995).

29) M. Yoshida, M. Lal, N. D. Kumar, P. N. Prasad, *J. Mater. Sci.*, **32**, 4047-4051 (1997).

30) S. Ando, Y. Watanabe, and T. Matsuura, *Jpn. J. Appl. Phys., Part 1*, **41**(8) 5254-5258 (2002).

31) J. Kobayashi, Y. Inoue, T. Matsuura, and T. Maruno, *IEICE Trans. Electron.*, **E81-C**, pp.1020-1026 (1998).

32) Y. Terui, S. Ando, *Prep. Jpn. Polyimide Conference*, **11**, 42 (2002).

33) Y. Terui and S. Ando, *Appl. Phys. Lett.*, **83**(23), 4755-4757 (2003).

34) *The following references are reviews of polymeric optical waveguides for telecommunication applications.*

a) A. Tomaru, *Optical Tech. Contact (Japanese)*, **36**(4), 23-33 (1998).

b) T. Maruno, *Applied Physics (Japanese)*, **68**(1), 4-13 (1999).

c) T. Maruno, *Technostream (Japanese)*, **24**(5), 28-32 (2001).

d) T. Maruno, *J. Electron. Inform. Comm. Soc. Jpn.*, **84**(9), 656-662 (2001).

e) N. Miyadera, *Hitachi Chemical Technical Report*, **37**(7), 7-16 (2001).

f) T. Kurihara, N. Ooba, S. Toyoda, T. Maruno, *Applied Physics (Japanese)*, **71**(12), 1508-1512 (2002).

g) J. Kobayashi, *J. Jpn. Electronics Mounting Society*, **5**(5), 500-506 (2002).

35) T. Oguchi, J. Noda, H. Hanafusa, and S. Nishi, *Electron. Lett.*, **27**, 706-707 (1991).

36) M. Kawachi, *Optical Quantum Electronics*, **22**, 391-416 (1990).

37) S. Ando, T. Sawada, and Y. Inoue, *Electron. Lett.*, **29**, 2143-2144 (1993).

38) T. Sawada, S. Ando, Y. Inoue, *Shingakugihou (Japanese)*, EDM94-39, CPM94-53, OPE94-48, 67-72 (1994).

39) Y. Inoue, H. Takahashi, S. Ando, T. Sawada, A. Himeno, and M. Kawachi, *IEEE J. Lightwave Technol.*, **15**, 1947-1957 (1997).

40) S. Ando, T. Sawada, and S. Sasaki, *Polym. Adv. Technol.*, **10**, 169-178 (1999).

41) S. Matsuda and S. Ando, *J. Polym. Sci., Part B: Polym. Phys.*, **41**(4), 418-428 (2003).

42) Y. Yasuda, S. Matsuda, and S. Ando (*submitted for publication*).

43) T. Sawada, S. Ando, H. Miyazawa, H. Takenaka and S. Sasaki, *Jpn. J. Appl. Phys.*, **37**, 6408-6413 (1998).

44) S. Ando, T. Sawada, and S. Sasaki, *Appl. Phys. Lett.*,

74, 938-940 (1999).

45) S. Matsuda, S. Ando, and T. Sawada, *Electron. Lett.*, **37**, 706-707 (2001).

46) S. Matsuda and S. Ando, *Polym. Adv. Technol.*, **14**, 458-470 (2003).

47) K. Furuya, B. I. Miller L. A. Coldren, and R. E. Howard, *Electron. Lett.*, **18**, 204-205 (1982).

48) T. C. Kowalczyk, T. Z. Kosc, K. D. Singer, A. J. Beuhler, D. A. Wargowski, P. A. Cahill, C. H. Seager, and M. B. Meinhardt, *Nonlinear Optics*, **14**, 185-195 (1995).

49) H. Franke, D. Wagner, T. Kleckers, R. Reuter, H. V. Rohitkumar, and B. A. Blech, *Applied Optics*, **32**, 2927-2935 (1993).

50) C. T. Sullivan, *Proc. SPIE*, **994**, 92-100 (1988).

51) T. Matsuura, S. Ando, S. Sasaki, and F. Yamamoto, *Electron. Lett.*, **29**, 269-270 (1993).

52) T. Matsuura, S. Ando, S. Matsui, S. Sasaki, and F. Yamamoto, *Electron. Lett.*, **29**, 2107-2108 (1993).

53) J. Kobayashi, T. Matsuura, T. Maruno, S. Sasaki, *Shingaku-gihou (Japanese)*, OME95-52, OPE95-93, 37-42 (1995).

54) T. Matsuura, J. Kobayashi, S. Ando, T. Maruno, S. Sasaki, and F. Yamamoto, *Applied Optics*, **38**, 966-971 (1999).

55) J. H. Kim, E. J. Kim, H. C. Choi, C. W. Kim, J. H. Cho, Y. W. Lee, B. G. You, S. Y. Yi, H. J. Lee, K. Han, W. H. Jang, T. H. Rhee, J. W. Lee, S. J. Pearton, *Thin Solid Films*, **341**, 192-195 (1999).

56) K. Han, W. Jang, and T. H. Rhee, *J. Appl. Polym. Sci.*, **77**, 2172-2177 (2000).

57) K. Han, H. Lee, and T. H. Rhee, *J. Appl. Polym. Sci.*, **74**, 107-112 (1999).

58) E. Kagei, N. Yamada, N. Kawakami, J. Kobayashi, T. Matsuura, F. Yamamoto, G. Masuda, K. Tajiri, M. Kuwabara, Y. Okumura, N. Asako, H. Yatani, *J. Electron. Inform. Comm. Soc. Jpn.*, **C-3-152**, 284 (2002).

59) A. J. Beuhler, D. A. Wargowski, K. D. Singer, and T. Kowalczyk, *IEEE Transactions on Components Packaging & Manufacturing Technology Part B-Advanced Packaging*, **18**, 232-234 (1995).

60) Y. Y. Maruo, S. Sasaki, and T. Tamamura, *IEEE J. Lightwave Technol.*, **13**, 1718-1723 (1995).

61) T. Maruno, T. Sakata, T. Ishii, Y. Y. Maruo, S. Sasaki, and T. Tamamura, "Organic Thin Films for Photonics Applications", **21**, *OSA Technical Digest Series*, p. 10-13 (1995).

62) T. Shiota, N. Takamatsu, *Prep. Jpn. Soc. Electron. Mountings*, **23C-13**, 337-338 (2000).

63) F. Shimokawa, S. Koike, and T. Matsuura, *Proc. 43rd Electron. Comp. & Technol. Conf.*, June 1-4, 705-710 (1993).

64) S. Koike, F. Shimokawa, T. Matsuura, and H. Takahara, *IEEE*, **19**, 124-130 (1996).

65) J. Kobayashi, T. Matsuura, S. Sasaki, T. Maruno, *Shingaku-gihou (Japanese)*, US97-28, EMD97-21, CPM97-43, OME97-49, 25-30 (1997).

66) M. Ukechi, T. Miyashita, R. Kaku, *Shingaku-Gihou (Japanese)*, EMD98-9, 19-24 (1998).

67) J. Kobayashi, T. Matsuura, S. Sasaki, and T. Maruno, *IEEE J. Lightwave Technol.*, **16**, 610-614 (1998).

68) K. Katada, T. Matsuura, H. Murakoshi, N. Yamada, F. Yamamoto, K. Uehara, J. Mizusawa, S. Sasaki, *Jpn. Soc. Electron. Inform. Comm., Prep. Elecron. Soc. Conf.*, **C-3-75**, 209 (1998).

69) E. Kagei, J. Kobayashi, N. Kawakami, A. Kudo, M. Hikita, A. Tomaru, K. Kurihara, T. Matusura, F. Yamamoto, *Prep. Jpn. Soc. Electron. Mounting*, **23C-12**, 335-336 (2000).

70) J. Kobayashi, Y. Inoue, T. Matsuura, and T. Maruno, *IEICE Trans. Electron.*, **81**, 1020-1026 (1998).

71) J. Kobayashi, T. Matsuura, Y. Hida, S. Sasaki, and T. Maruno, *IEEE J. Lightwave Technol.*, **16**, 1024-1029 (1998).

72) H. Masuda, T. Shibata, T. Ido, M. Takahashi, *Hitachi Chemical Technical Report*, **39** (7), 37-40 (2002).

73) D. Fujita, T. Sakuma, H. Hosoya, *J. Jpn. Soc. Electron. Inform. Comm.*, **C-3-67**, 232 (2001).

74) M. C. Oh, M. H. Lee, and H. J. Lee, *IEEE Photon. Tech. Lett.*, **11**, 1144-1146 (1999).

75) T. Ido, A. Kuwabara, T. Nagara, H. Ichikawa, M. Tokuda, T. Kinoshita, S. Tshuji, H. Sano, *Shingaku-Gihou (Japanese)*, EMD99-24, CPM99-56, OPE99-46, LQE99-40, 7-12 (1999).